Electronic Supplementary Material (ESI) for Chemical Science.

Supplementary Information

BPTI folding revisited: switching a disulfide bond into methylene thioacetal reveals a previously hidden path

Reem Mousa, Shifra Lansky, Gil Shoham and Norman Metanis*

The Institute of Chemistry,

The Hebrew University of Jerusalem, Edmond J. Safra, Givat Ram,

Jerusalem 91904, Israel

metanis@mail.huji.ac.il

Materials and Methods

Buffers for all kinetic experiments were prepared using MilliQ water (Millipore, Merck). $Na_2HPO_4 \cdot 12H_2O$, tris(2-carboxyethyl)phosphine hydrochloride (TCEP·HCl), *DL*-dithiothreitol (DTT), diiodomethane, bovine α-chymotrypsin and *N*-succinyl-Gly-Gly-Phe-*p*-nitoanilide substrate were purchased from Sigma-Aldrich. Ultrapure guanidinium chloride (Gn·HCl, MP Biomedicals, LLC, France) was used for unfolding experiments. Bovine pancreatic trypsin inhibitor (WT-BPTI) was a generous gift of Bachem AG. All solvents: Dimethyl sulfoxide (DMSO), acetonitrile (ACN), methanol and trifluoroacetic acid (TFA) were HPLC or UPLC grade and were purchased from Bio-Lab, Jerusalem.

High Performance Liquid Chromatography (HPLC)

The analytical analyses were performed on a reverse-phase Waters Alliance HPLC with UV detector (214 or 220 nm, and 280 nm) using an X-Bridge C4 column (3.5 μm, 4.6 × 150 mm) and an Atlantis T3 column (3 μm, 4.6 × 150 mm). Semi-preparative RP-HPLC was performed on a Waters LCQ150 system using X-Bridge C8 column (5 μm, 10 × 150 mm) or X-Bridge BEH300 C4 (5 μm 19 × 150 mm), accordingly. Linear gradients of acetonitrile with 0.1% TFA (buffer B) and water with 0.1% TFA (buffer A) were used for all systems to elute bound peptides. The flow rates were 1 mL/min (analytical), 3.35 and 10 mL/min (semi-preparative).

Electrospray Ionization Mass Spectrometry (ESI-MS) and HR-MS

ESI-MS was performed on Thermo Scientific-LCQ Fleet Ion-Trap mass spectrometer. Peptide masses were calculated from the experimental mass to charge (m/z) ratios from the observed multiply charged species of a peptide using MagTran v1.03.

The HR-MS were recorded on a Q-ExactivePlus Orbitrap mass spectrometer (Thermo Scientific) with a ESI source and 140’000 FWHM, in a method with AGC target set to

1E6, and scan range was 400-2800 m/z. The raw data was deconvoluted by MagTran v1.03 software.

Experimental Section

Preparation of reduced WT-BPTI and reduced MT-BPTI

Native, folded WT-BPTI (15 mg, 2.3 μmol) was dissolved in sodium phosphate buffer (100 mM, pH ~8) and treated with 1.5 equiv of TCEP. Within 3 h, the solvent exposed disulfide bond 14–38 was selectivity reduced.[1, 2] The reaction progress was monitored by ESI-MS and HPLC (X-Bridge C4 column, 3.5 μm, 4.6 × 150 mm) using a gradient of 15:85 to 60:40 (0.1% Buffer B: Buffer A) over 25 min. Upon completion of the reduction step, 100 fold excess of diiodomethane in DMSO was added to the reaction and stirred at 35 °C under argon.[3] After 22 h the reaction was quenched with 0.1% TFA in water and purified by preparative RP-HPLC (X-Bridge BEH300 C4 column, 5μm, 19 × 150 mm) using a gradient of 15:85 to 50:50 (B: A) over 50 min. In addition to the formation of the MT-BPTI (10 mg isolated, 70% yield), regeneration of 14–38 disulfide bond to form folded WT-BPTI was observed as a minor product (~8 %). The protein was dissolved in 200 mM sodium phosphate buffer, with 6 M Gn·HCl, pH 7.2, and reduced with 200 equiv of DTT at 55 °C for 3 h. The reaction solution was injected into an X-Bridge BEH300 C4 column (5μm, 19 × 150 mm) and eluted using the same method mentioned before. The pure, reduced MT-BPTI was isolated in 50% yield (5 mg). Both reduced WT-BPTI and reduced MT-BPTI fractions were lyophilized subsequently and dissolved in 10 mM HCl to a concentration of 546 μM and 526 μM, respectively. The concentration of the proteins was determined by Thermo Scientific Evolution™ 201 UV-Visible spectrophotometer. ε_{280} of WT-BPTI analogs is 5400 $cm^{-1}M^{-1}$.

To produce the reduced WT-BPTI, 10 mg (1.5 μmol) of folded WT-BPTI was dissolved in 200 mM sodium phosphate, containing 6 M Gn·HCl, at pH 7.2 in the presence of 200 equiv of DTT. Within 5 h the reaction was quenched with 0.1% TFA in water and injected into an X-Bridge BEH300 C4 column (5 μm, 19 × 150 mm) for purification as described above, and the reduced WT-BPTI was eluted and lyophilized in 50% yield (5 mg).

Oxidative folding of reduced WT-BPTI and reduced MT-BPTI (standard conditions)

The oxidative folding experiments performed according to the work of Weissman and Kim.[4-6] The folding reactions were performed in an anaerobic chamber (Coy Laboratories Inc.) under nitrogen and hydrogen atmosphere (95%:5%) in degassed phosphate buffer (100 mM sodium phosphate, 150 mM NaCl, 1 mM EDTA, pH 7.3) or Tris·HCl buffer (100 mM Tris·HCl, 200 mM KCl, 1mM EDTA, pH 8.7). Oxidized glutathione (GSSG, 5 equiv, final concentration 150 μM for WT-BPTI and 100 μM for MT-BPTI) was added to 30 μM of reduced WT-BPTI and 20 μM of reduced MT-BPTI, respectively. At various time intervals, 80 μL aliquots were removed and quenched with 30 μL of 2 M HCl, and stored at -20°C before analysis by analytical HPLC. The reaction mixture was injected into Atlantis T3 column (3 μm 4.6 × 150 mm heated to 40°C) and eluted from the column by 10:90 to 26.5:73.5 gradient over 5 min (B:A), and increasing to 40:60 over 20 min. All chromatograms were monitored at a wavelength of 214 nm.

Oxidative folding of reduced WT-BPTI and reduced MT-BPTI with 25 equiv GSSG

The two reduced proteins were folded under similar conditions mentioned above except that here we used larger excess of GSSG (25 equiv relative to the protein concentration; final concentration 750 μM for WT-BPTI and 500 μM for MT-BPTI), with 30 μM of reduced WT-BPTI and 20 μM of reduced MT-BPTI, respectively. The reaction was performed in an anaerobic chamber as described before, and at time intervals 80 μL aliquots were removed and quenched with 30 μL 2 M HCl. The samples were stored at -20°C until subjected to analytical HPLC.

Isolation of MT-N' and MT-N* intermediates

Reduced MT-BPTI (2 mg, 0.3 μmol) was dissolved in 10 mM HCl and added to phosphate buffer (100 mM sodium phosphate, 150 mM NaCl, 1 mM EDTA, pH 7.3) to final concentration of 20 μM, and in the presence of GSSG to a final concentration 100 μM. The folding reaction was quenched with 2 M HCl after 240 min (at this time point

MT-N' and MT-N* are the major species). The separation of the two intermediates was done by analytical HPLC.

Rearrangement of MT-N' and MT-N* intermediates

For the rearrangement experiment, purified intermediates MT-N' and MT-N* were separately dissolved in degassed Tris-HCl buffer (100 mM Tris-HCl, 200 mM KCl, 1 mM EDTA, pH 8.7) to a final concentration of 15 µM in 500 µL, in the absence of GSSG. The reaction was carried out in an anaerobic chamber under a mixture of hydrogen and nitrogen. At time intervals, 80 µL aliquots were removed and quenched with 30 µL 2 M HCl. The samples were stored at -20°C until subjected to analytical HPLC as described above.

Stability experiments of folded WT-BPTI and folded MT-BPTI

WT-BPTI (1 mg, 0.15 µmol) and MT-BPTI (0.5 mg, 0.08 µmol) were dissolved in 200 mM phosphate buffer pH 7, in the presence of 2 M of Gn·HCl, and 100 equiv of DTT was added to the solution. The experiment was done under aerobic conditions at room temperature. At time intervals, 80 µL aliquots were removed and quenched with acid. The reaction was monitored by analytical HPLC, using Atlantis T3 column (3 µm 4.6 × 150 mm, at 40°C), and eluted by 10:90 to 26.5:73.5 to 40:60 over 27 min gradient (B:A).

Circular dichroism (CD)

The secondary structures of the folded proteins WT-BPTI and MT-BPTI were compared using CD spectroscopy, in the far-UV range (190 nm to 250 nm). CD measurement was performed at 25 °C in 10 mM sodium phosphate buffer, pH 7, in a 0.1 cm cuvette using MOS-500 spectropolarimeter (BioLogic). Protein concentrations were 55.5 µM for WT-BPTI and 48.5 µM for MT-BPTI, respectively. The spectra were recorded by averaging 5 wavelength scans in 1 nm steps, with a signal averaging time of 0.05 s and a bandwidth of 2 nm.

$$[\Theta]_{MER} = \frac{\Theta(mdeg)}{10 \times l\,(cm) \times c(M) \times N(\#amide\ bonds)}$$

Inhibition assays

The chymotrypsin inhibition assay[7] was tested with *N*-succinyl-Gly-Gly-Phe-*p*-nitroanilide (SucGGF*p*NA) substrate, in Tris-HCl buffer (50 mM, 20 mM $CaCl_2$, 0.05% triton X-100, pH 8.2) at 25 °C. Protein concentration was determined by spectrophotometer (ε_{280} of α-chymotrypsin is 49600 $cm^{-1}M^{-1}$;[8] ε_{280} of WT-BPTI analogs is 5400 $cm^{-1}M^{-1}$). The initial rate of *p*-nitroaniline formation was followed at 405 nm (ε_{405}=8270 $cm^{-1}M^{-1}$) using a Thermo Scientific Evolution™ 201 UV-Visible spectrophotometer. For the inhibition assay, 42 nM of α-chymotrypsin and 40 μM SucGGF*p*NA substrate were incubated with inhibitor (WT-BPTI or MT-BPTI). The initial rates (v_0) were measured at concentrations of inhibitor varying from 0-80 nM, and were fitted to the following inhibition equation to calculate K_i:[9]

$$v = \frac{v_0}{2\alpha E}\left(\alpha E - I - K_i\right) + \sqrt{\left(K_i + \alpha E - I\right)^2 + 4K_i I}$$

The observed K_i values for WT-BPTI (12.7 ± 0.8 nM) and MT-BPTI (12.6 ± 0.7 nM) are practically identical within experimental error and with excellent agreement with previous literature (11 nM).[7]

X-ray crystallography.

Lyophilized MT-BPTI was dissolved in triple distilled water to obtain a ~9 mg/ml solution, which was used subsequently for crystallization experiments. Optimal crystals of MT-BPTI were obtained by the hanging-drop vapor diffusion method, using 2 μL drops with a 1:1 ratio between protein and reservoir, equilibrated over a 500 μL reservoir solution containing 1.7 M $(NH_4)_2SO_4$. These crystals appeared after 2-3 days and grew to their final size in a week. They were soaked for ~15 sec in a solution containing 25% glycerol and 75% reservoir prior to their flash-freezing in liquid nitrogen for X-ray diffraction data collection.

X-ray diffraction data were collected for one of these MT-BPTI crystals, using an Eiger X 4M detector, at the ID30A-3 beamline (λ=0.964 Å, T=100 K) of the ESRF synchrotron (Grenoble, France). The raw diffraction images were processed, integrated, and scaled with the XDS software,[10] confirming a complete data set at 1.72 Å resolution belonging

to the $P6_422$ space group (Table S1). These data allowed a straightforward structure determination of MT-BPTI by molecular replacement, using the program Phaser[11] and the native WT-BPTI structure (pdb code 2HEX[12]) as search model, with five MT-BPTI monomers in the asymmetric unit. Modeling of the MT-BPTI structure was conducted with the program Coot,[13] which included the modeling of the 14–38 MT bridge in two alternate conformations, and the addition of sulfate and glycerol molecules resulting from the crystallization and cryo-protectant solutions. This manual building was accompanied by iterative cycles of concomitant refinement with phenix.refine,[14] resulting in a final structure with R_{work} and R_{free} values of 18.91% and 20.73%, respectively. Geometric validation of the structure was conducted with Procheck[15] and Molprobity[16], confirming a model of good structural and stereochemical parameters, as demonstrated by root mean square deviation (RMSD) values of 0.01 Å and 1.5° for bond lengths and bond angles, respectively. The final MT-BPTI structure has been deposited in the RCSB protein data bank[17] under accession code **6F1F**. Further details regarding data collection, data processing, structure determination and refinement of the MT-BPTI structure are listed in Table S1.

Supplementary Figures, Schemes and Tables

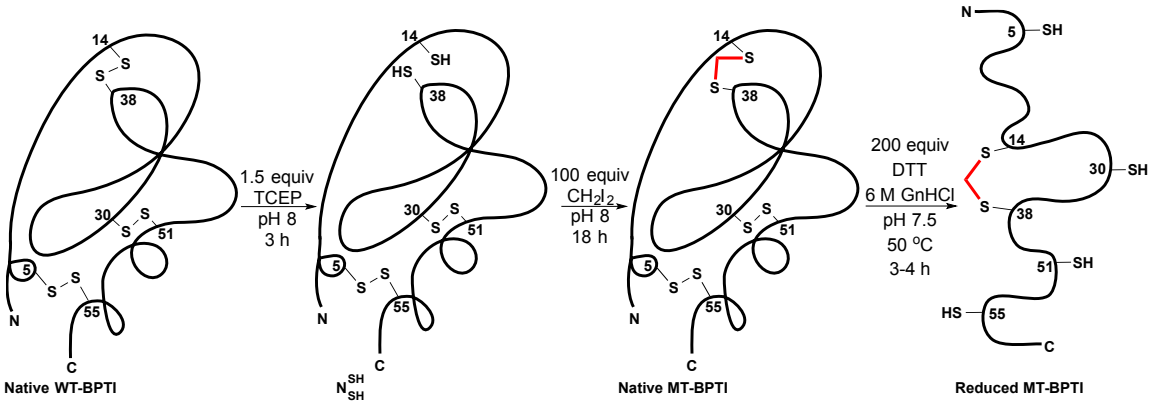

Figure S1. Schematic representation for the preparation of reduced MT-BPTI.

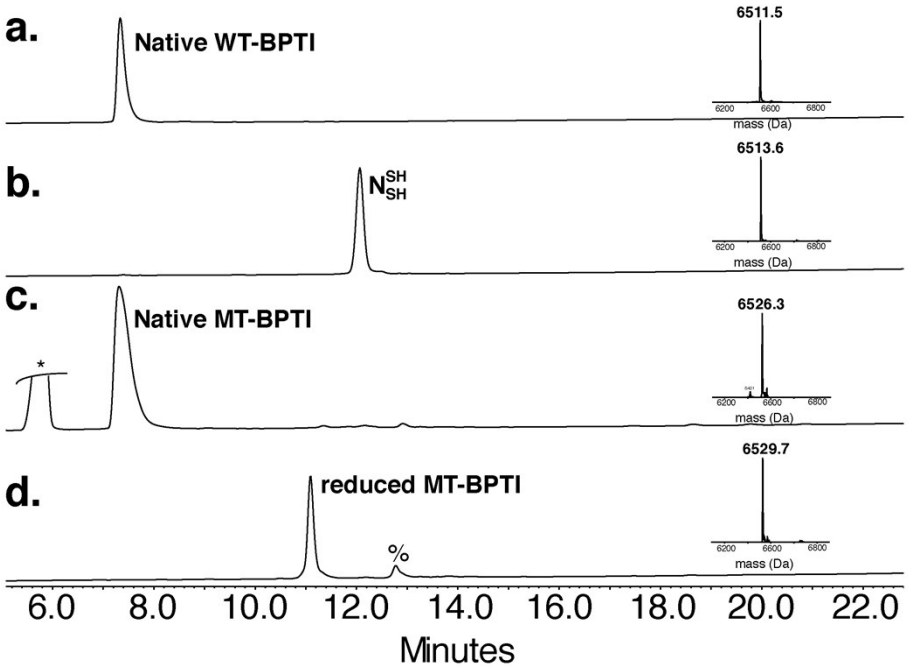

Figure S2. Preparation of reduced MT-BPTI. **a**. Folded WT-BPTI (mass: expected 6511.50, observed 6511.5 ± 1.1 Da); **b**. Selective reduction of 14-38 disulfide bond by TCEP to form N^{SH}_{SH} [5-55, 30-51] (mass: expected 6513.5, observed 6513.6 ± 0.4 Da); **c**. Alkylation of N^{SH}_{SH} by diiodomethane in DMSO to form MT-BPTI (mass: expected 6525.5, observed 6526.3 ± 0.7 Da). (*) is small molecule byproduct of the reaction; **d**. Reduced MT-BPTI (mass: expected 6529.6, observed 6529.7 ± 0.4 Da) with four free Cys5/30/51 and 55, prepared by reduction with large excess of DTT at 55 °C. (%) is traces of reduced WT-BPTI.

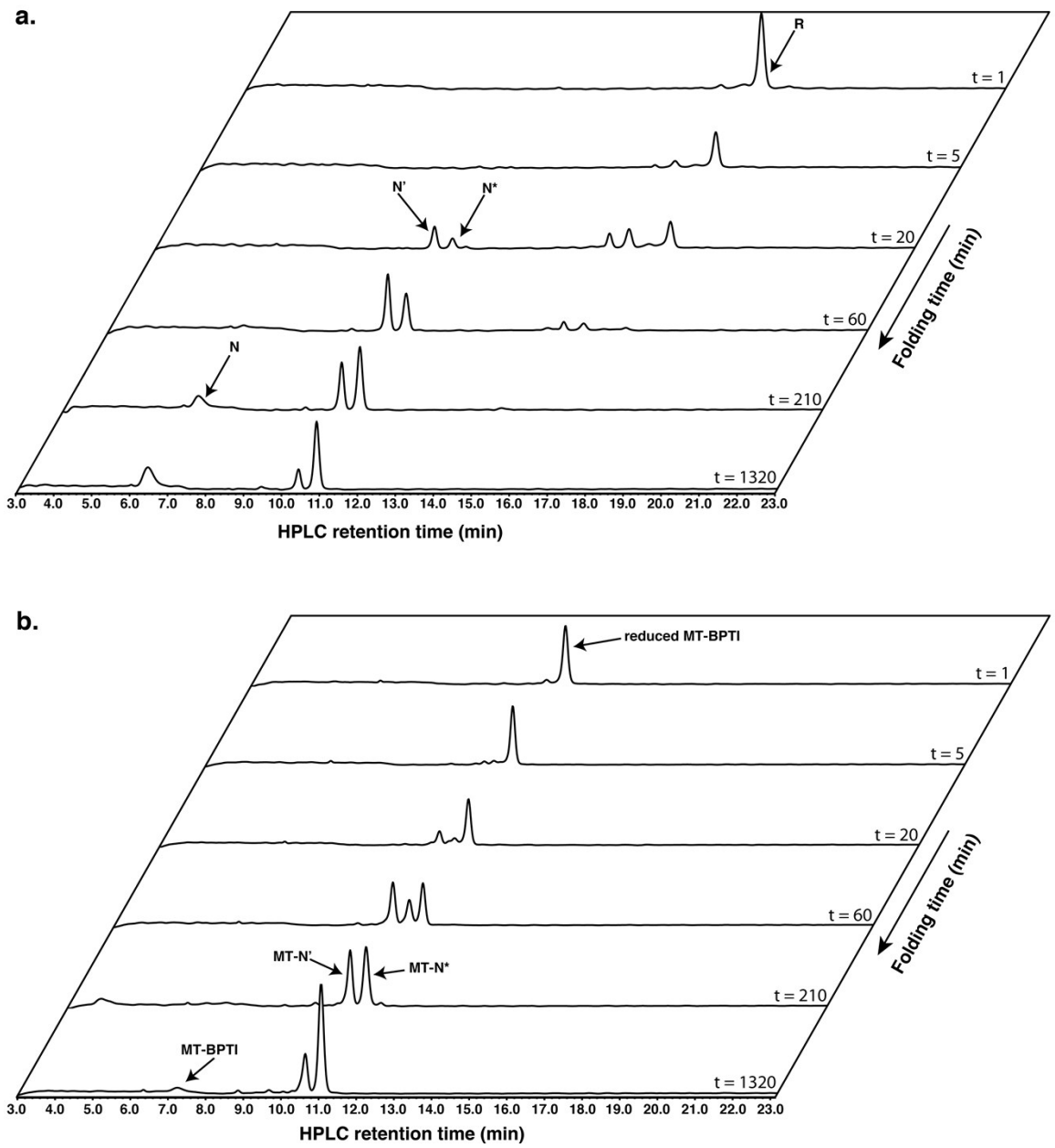

Figure S3. Anaerobic oxidative folding at pH 7.3 of **a**. 30 μM reduced WT-BPTI with 150 μM GSSG and **b**. 20 μM reduced MT-BPTI with 100 μM GSSG.

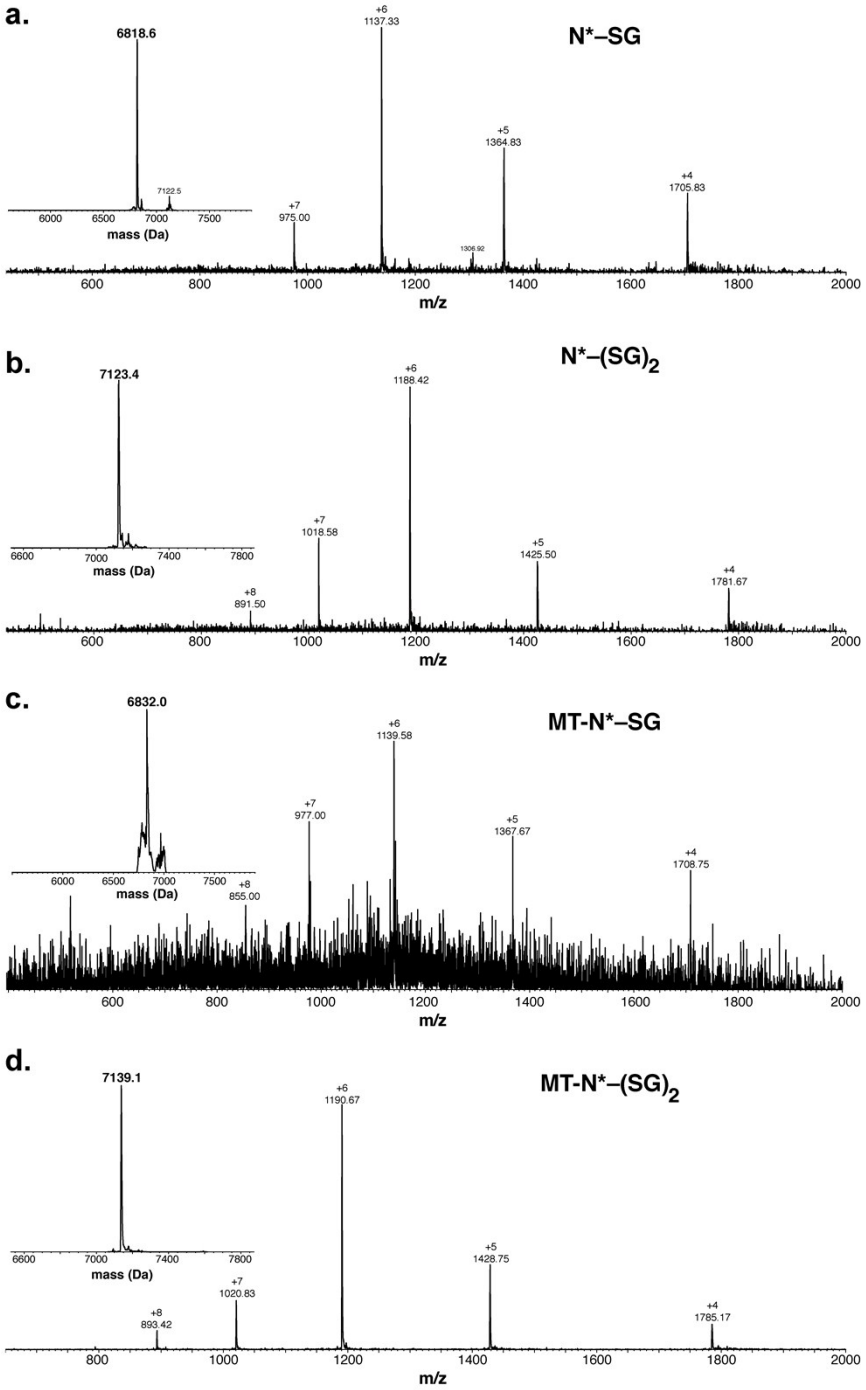

Figure S4. Glutathionylated intermediates of N* and MT-N* observed during the oxidative folding of WT-BPTI and MT-BPTI. **a**. ESI-MS of isolated N*–SG appears at R_t = 9.8 min, inset obs. mass 6818.6 ± 0.7, calc. 6818.8 Da; **b**. ESI-MS of isolated N*–**(**$SG)_2$ appears at R_t = 8.7 min, inset obs. mass 7123.4 ± 0.9, calc. 7124.2 Da; **c**. ESI-MS of isolated MT-N*–SG appears at R_t = 9.9 min, inset obs. mass 6832.0 Da ± 0.9, calc. 6832.9 Da; **d**. ESI-MS of isolated MT-N*–**(**$SG)_2$ appears at R_t = 8.8 min, inset obs. mass 7139.1 Da ± 1.0, calc. 7138.2 Da.

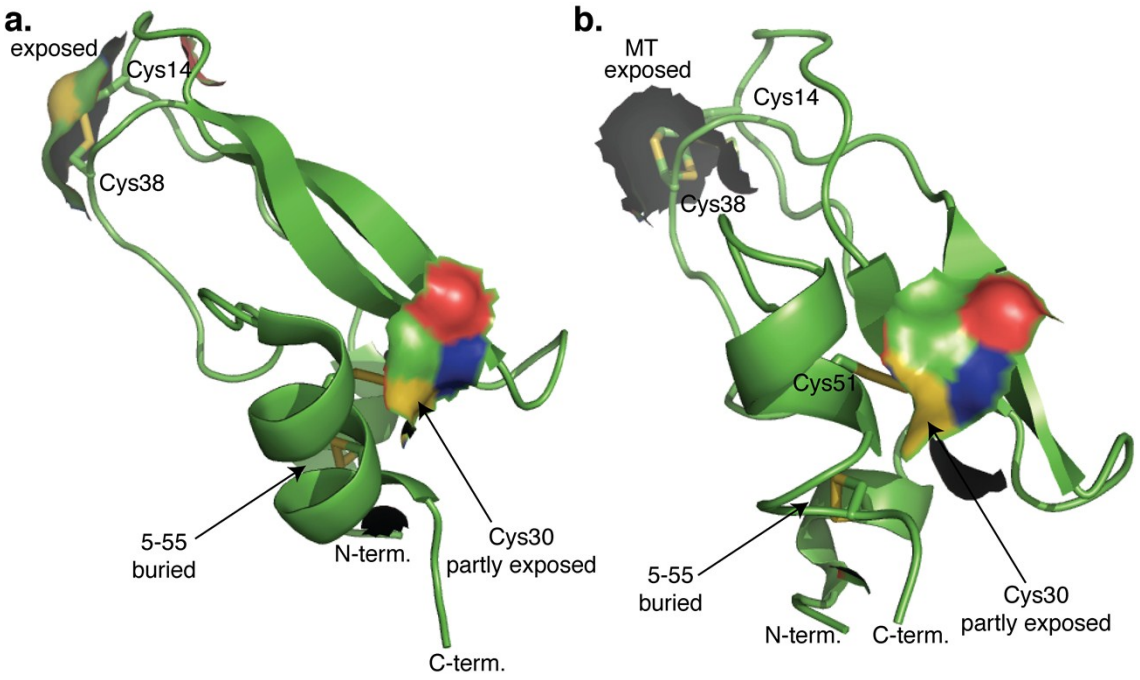

Figure S5. Analysis of the surface area around the disulfide bonds and MT moiety in the structures of **a**. WT-BPTI (PDB:1BPI) and **b**. MT-BPTI (PDB: 6F1F). Both structures indicate the 14–38 disulfide/MT crosslinks are solvent exposed while 5–55 is buried. Cys30 in both structures is partly solvent exposed and hence suggested to react with GSSG in N* to give N*–SG and MT-N*–SG intermediates.

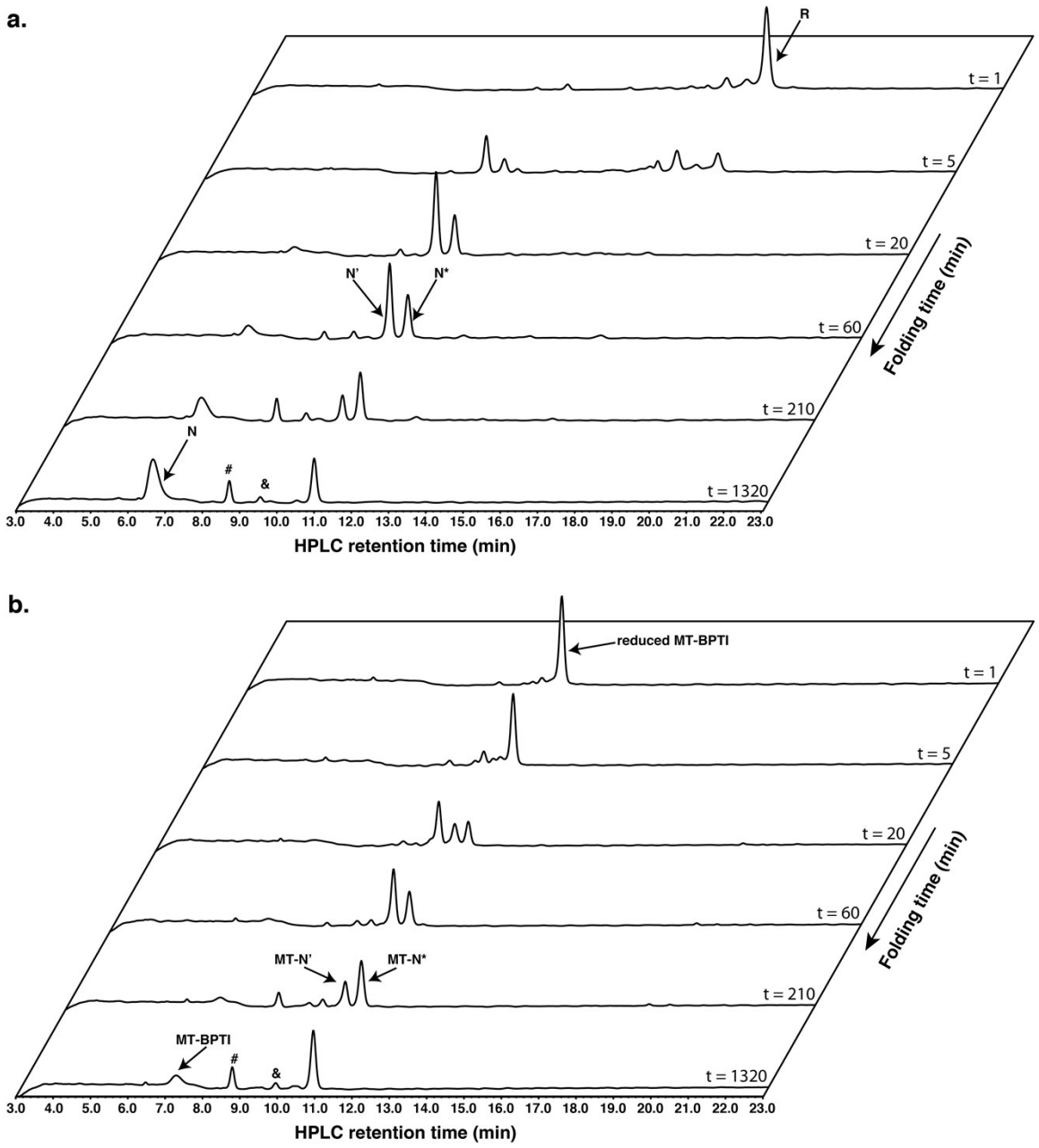

Figure S6. Anaerobic oxidative folding at pH 7.3 of **a**. 30 μM reduced WT-BPTI with 750 μM GSSG and **b**. 20 μM reduced MT-BPTI with 500 μM GSSG. & and # signs are MT-N*–SG and MT-N*–$(SG)_2$, respectively.

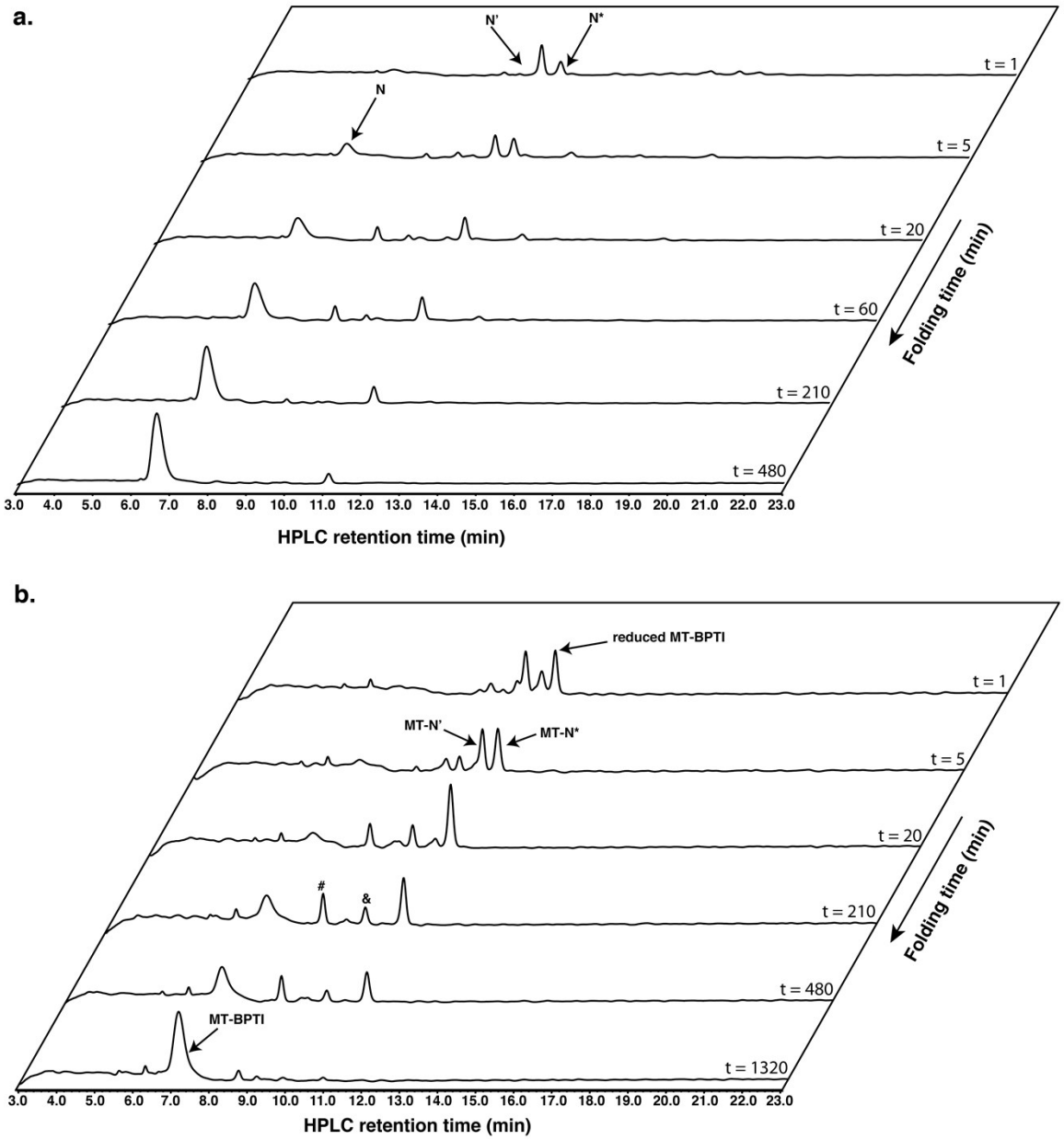

Figure S7. Anaerobic oxidative folding at pH 8.7 of **a**. 30 μM reduced WT-BPTI with 750 μM GSSG and **b**. 20 μM reduced MT-BPTI with 500 μM GSSG. & and # signs are MT-N*–SG and MT-N*–$(SG)_2$, respectively.

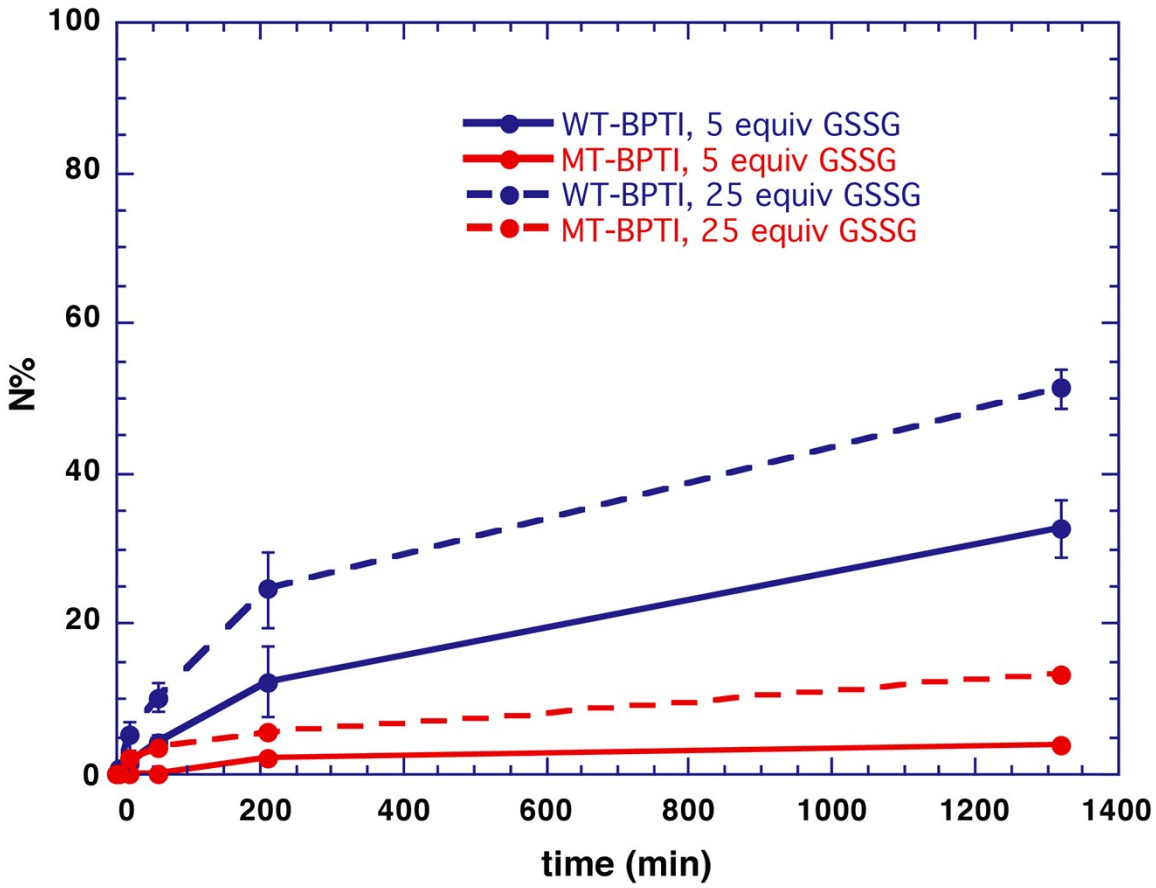

Figure S8. Kinetic traces of the oxidative folding reactions at pH 7.3 of reduced WT-BPTI (*blue*) and reduced MT-BPTI (*red*), in the presence of 5 equiv (*solid*) or 25 equiv (*dashed*) GSSG. The s.d. values were calculated from experiments done in triplicate and the lines connecting the data points are shown only for clarity and do not represent a data fit.

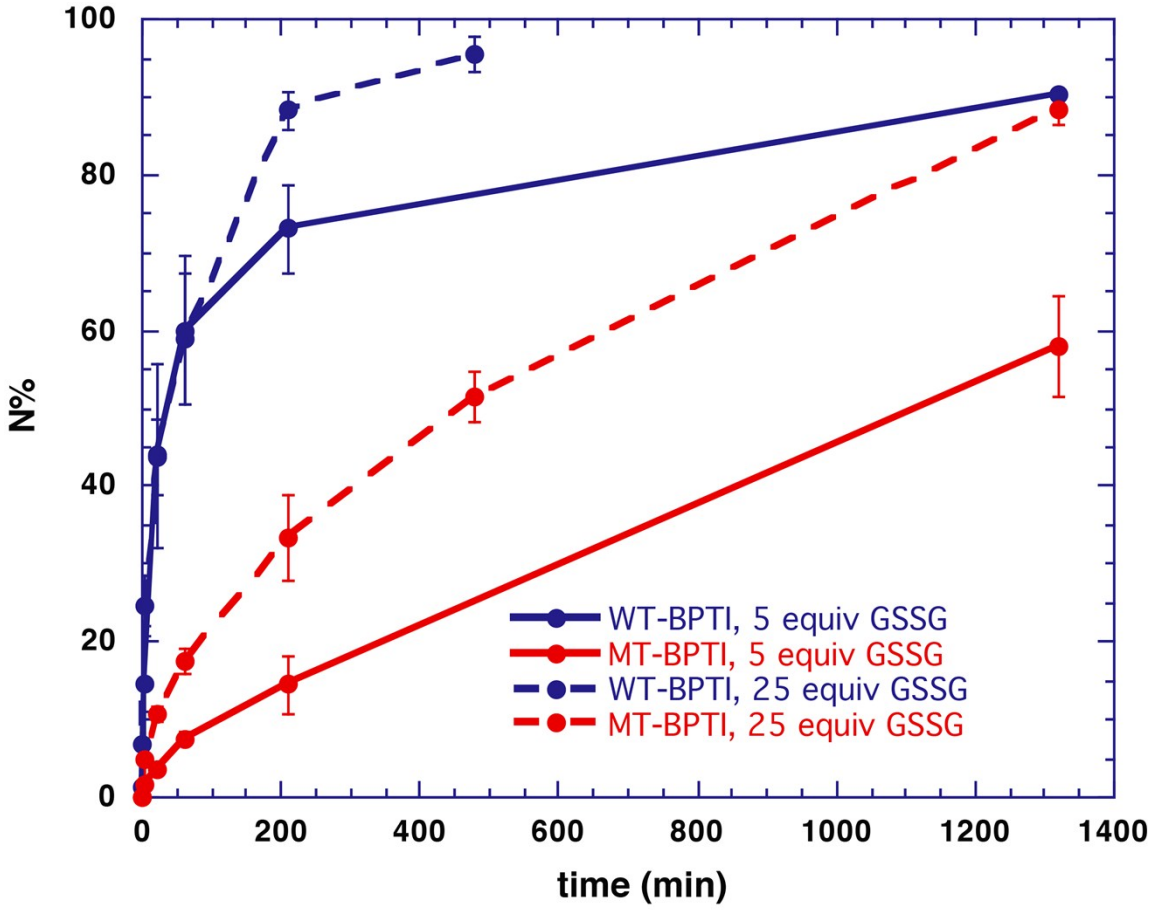

Figure S9. Kinetic traces of the oxidative folding reactions at pH 8.7 of reduced WT-BPTI (*blue*) and reduced MT-BPTI (*red*), in the presence of 5 equiv (*solid*) or 25 equiv (*dashed*) GSSG. The s.d. values were calculated from experiments done in triplicate and the lines connecting the data points are shown only for clarity and do not represent a data fit.

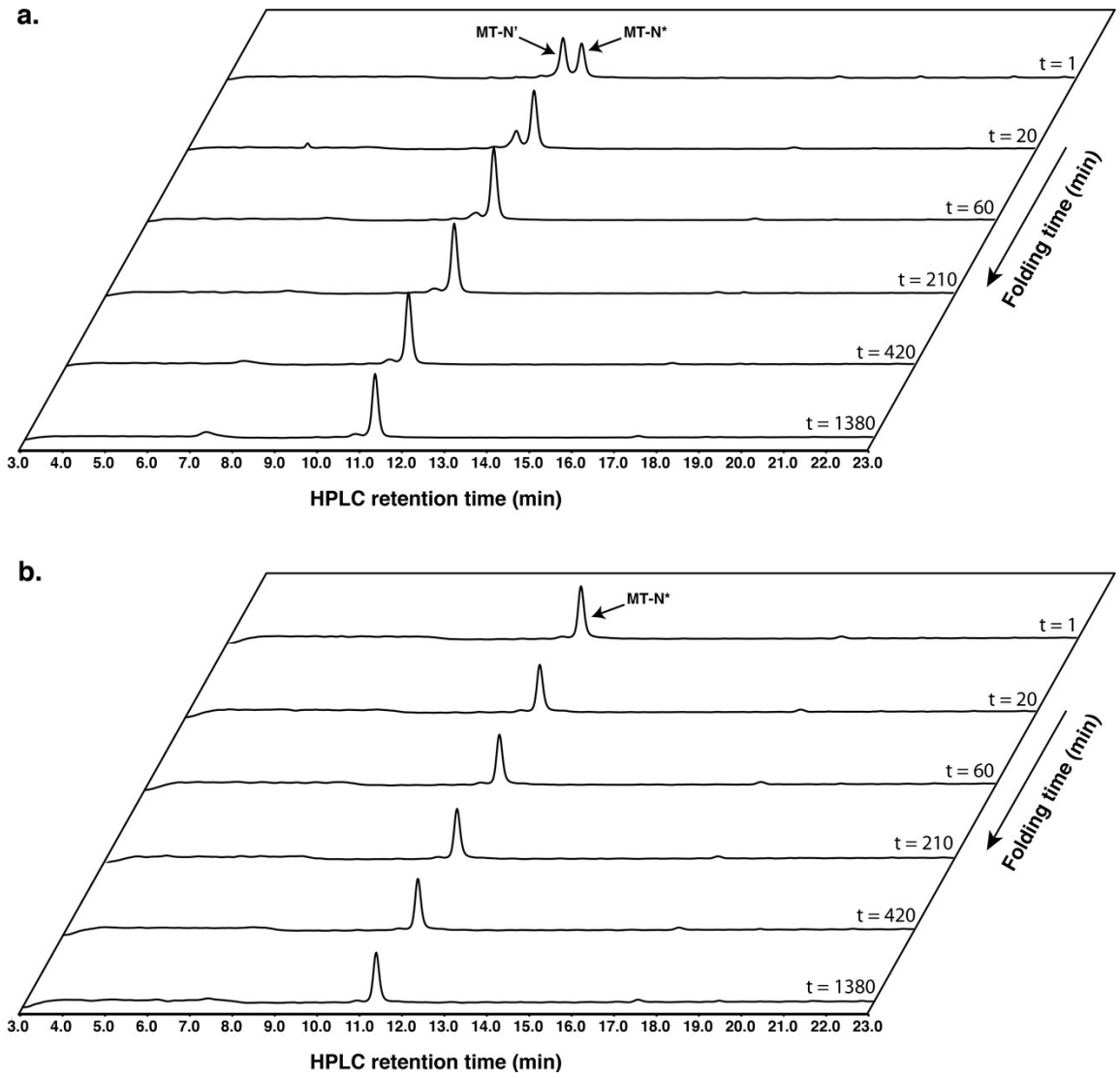

Figure S10. Rearrangement at pH 8.7 of **a**. 15 μM of MT-N' and **b**. 15 μM of MT-N* in the absence of oxidizing agent GSSG.

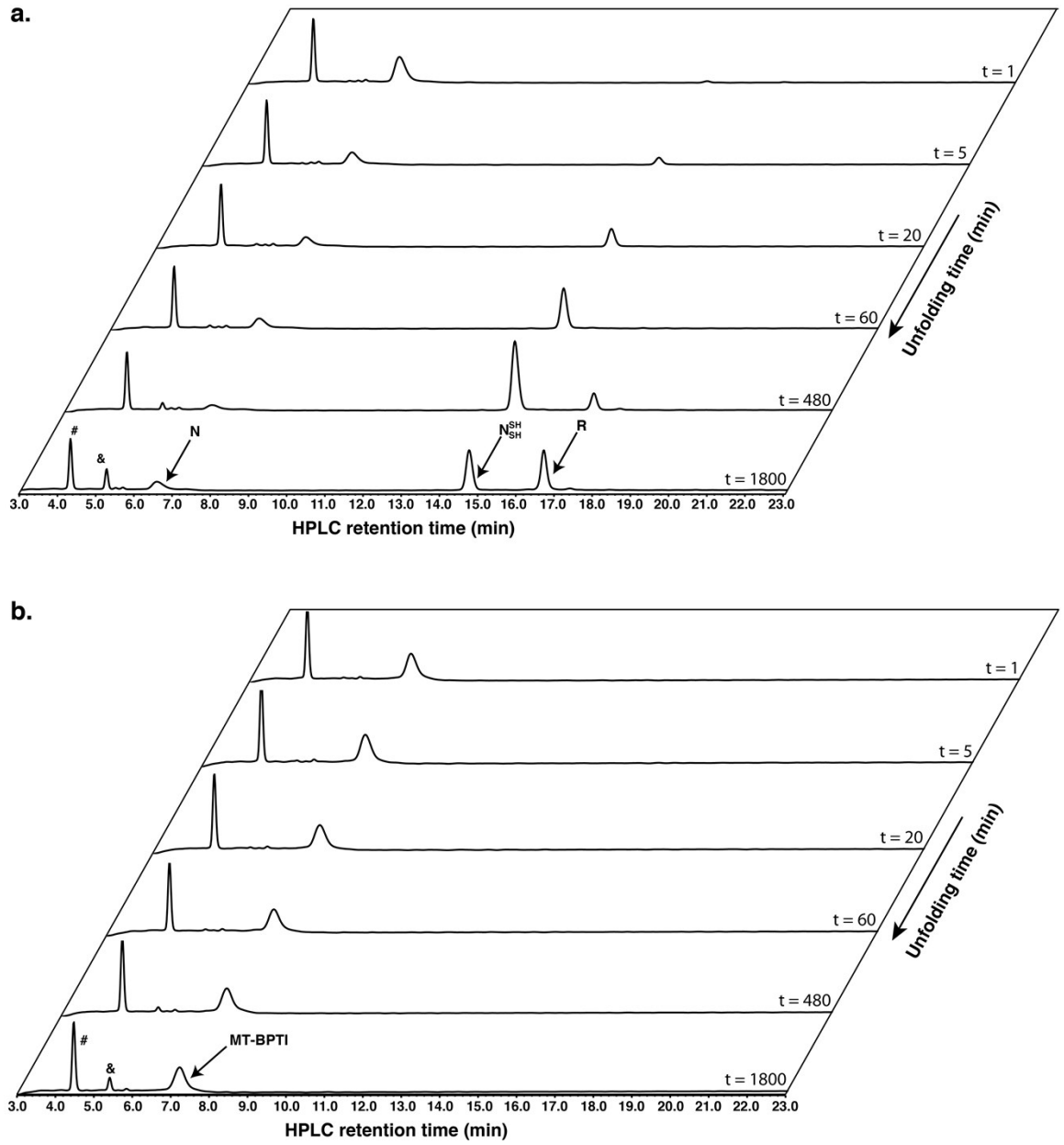

Figure S11. The reductive unfolding at pH 7 in the presence of 2 M of Gn·HCl and 100 equiv of DTT of **a**. 30 μM of WT-BPTI and **b**. 30 μM of MT-BPTI, # and & signs are reduced and oxidized DTT, respectively.

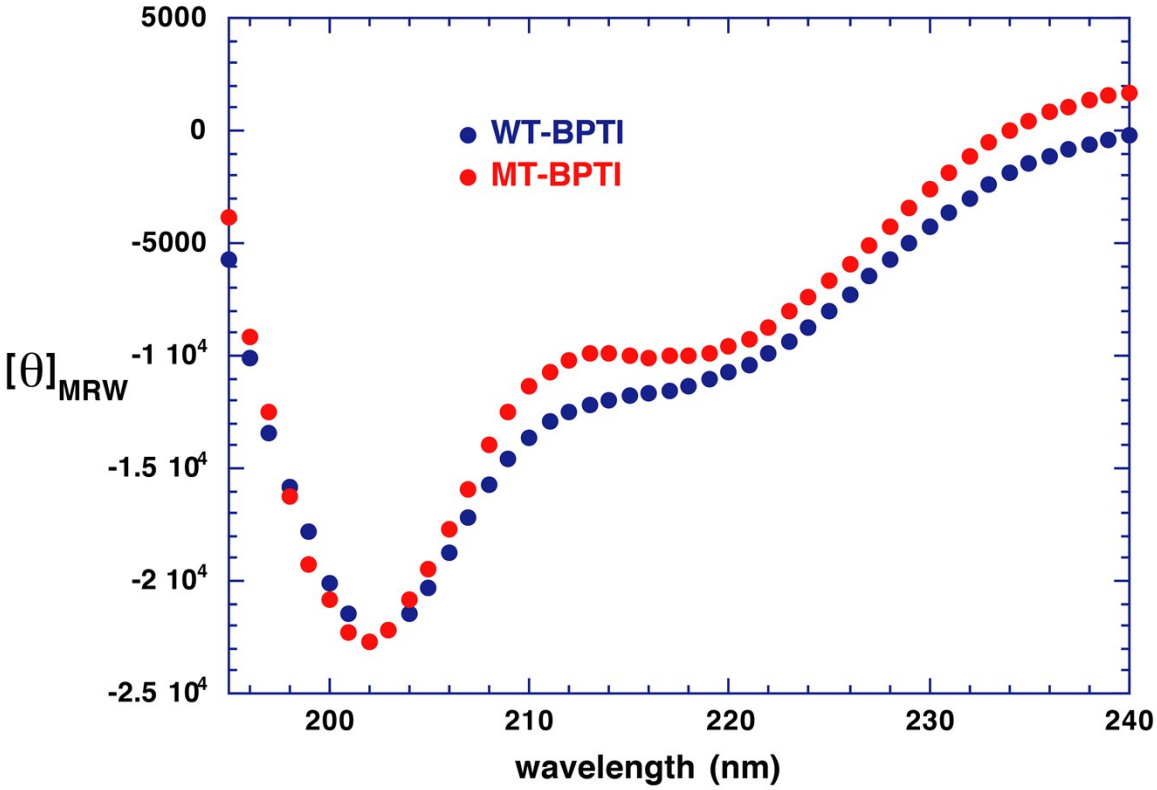

Figure S12. Far-UV CD spectra of WT-BPTI and MT-BPTI. WT-BPTI (55.5 μM) and MT-BPTI (48.5 μM) were each dissolved in degassed 10 mM PBS, pH 7.

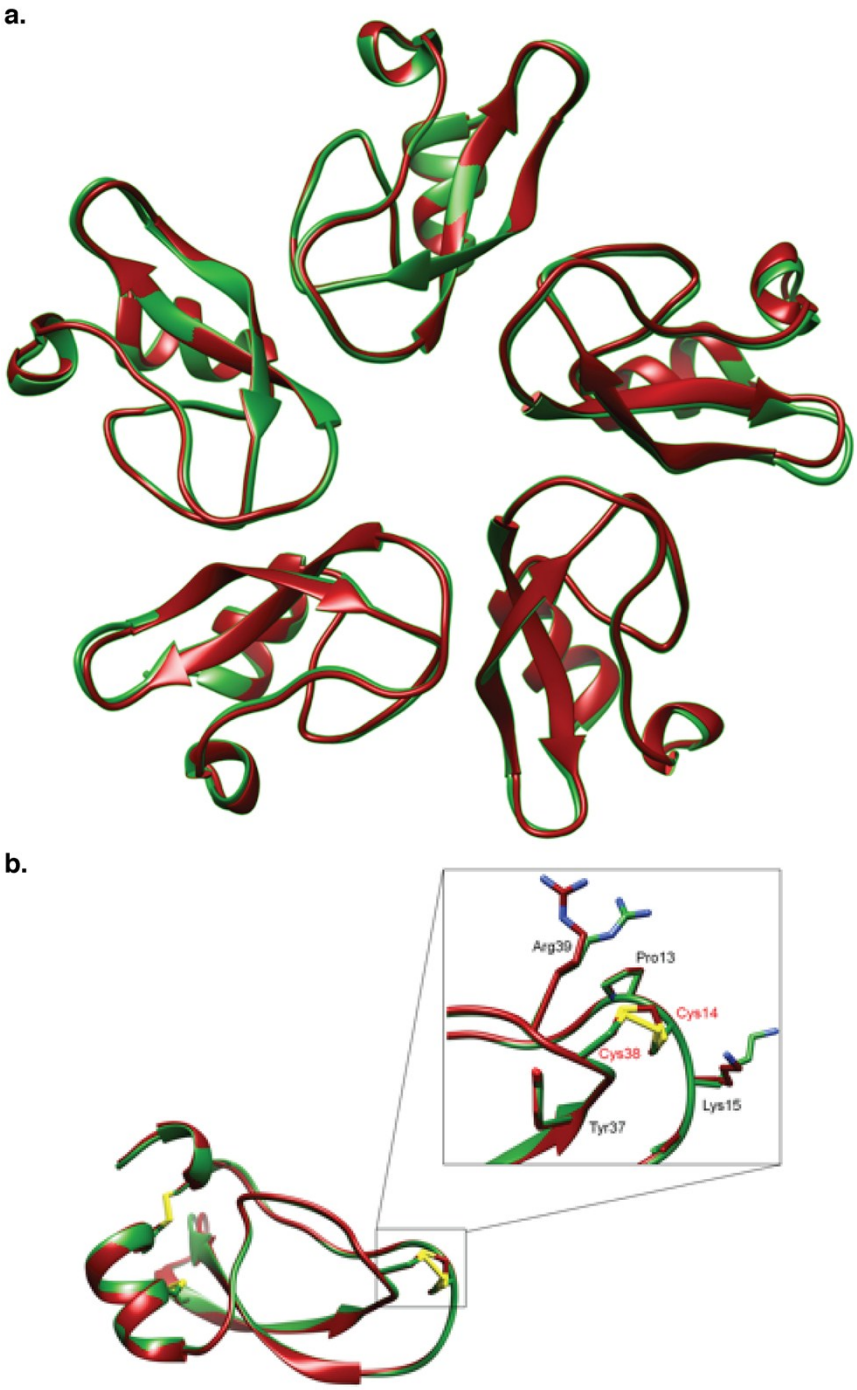

Figure S13. Crystal structure comparisons between WT-BPTI (PDB code 2HEX, *green*) and MT-BPTI (6F1F, *dark red*). **a**. The pentameric assembly observed in the asymmetric unit. **b**. The monomeric structure showing minor conformational changes in the backbone and side chains as a result of the MT substitution. For the sake of clarity, only one conformation for the MT bridge is shown.

Table S1: Data collection and processing details for the MT-BPTI structure

Structure determination and refinement	
Data collection and processing	
X-ray Source	ESRF ID30A-3
Processing software	XDS
Space group	$P6_422$
Wavelength (Å)	0.968
Rotation range (°)	360
Oscillation range $\Delta\phi$ (°)	0.1
a = c (Å) b (Å)	95.51 157.13
Resolution range (Å)	47.77-1.72
No. of reflections: total unique	 1,819,171 45,433
Multiplicity	40.0 (39.9)
$\langle I/\sigma(I)\rangle$	34.98 (2.25)
Mosaicity (°)	0.124
Completeness (%):	98.9 (93.3)
R_{merge} (%) **	7.4 (173.9)
$CC_{1/2}$	1.00 (0.89)
Resolution range (Å)	47.75-1.72
R_{factor} (%)†	18.91
(no. of reflections)	43,036
R_{free} (%)††	20.73
(no. of reflections)	2,267
Refined model No. of chains in AU No. of residues No. of atoms No. of water molecules	 5 228 2769 222
<B> factor (Å^2)	38.9
Ramachandran plot Favored (%) Allowed (%) Disallowed (%)	 98.1 1.9 0.0
RMS deviation Bond lengths (Å) Bond angles(deg.)	 0.011 1.548
PDB code	**6F1F**

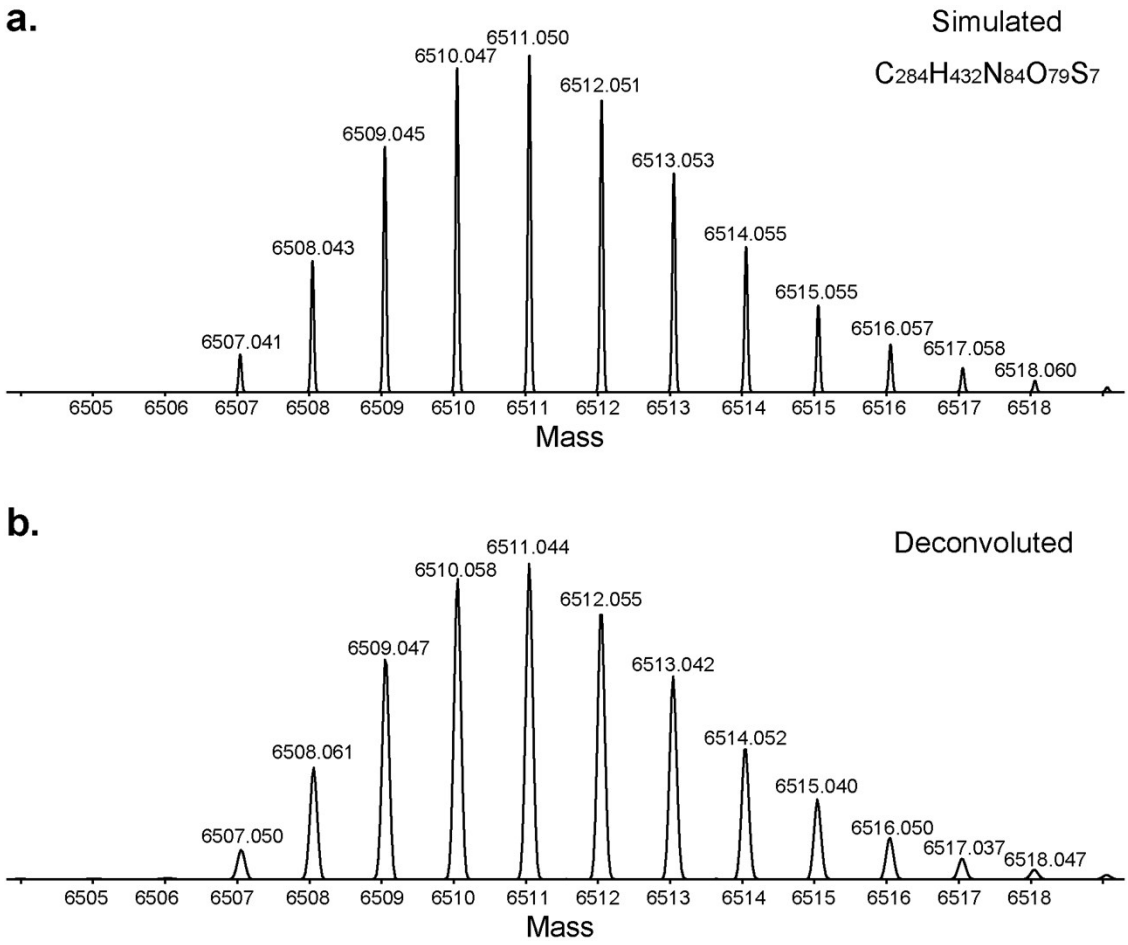

Figure S14. HR-MS analysis of WT-BPTI. **a**. The simulated HR-MS of folded WT-BPTI with chemical formula $C_{284}H_{432}N_{84}O_{79}S_7$ is shown; **b**. The deconvoluted HR-MS of WT-BPTI.

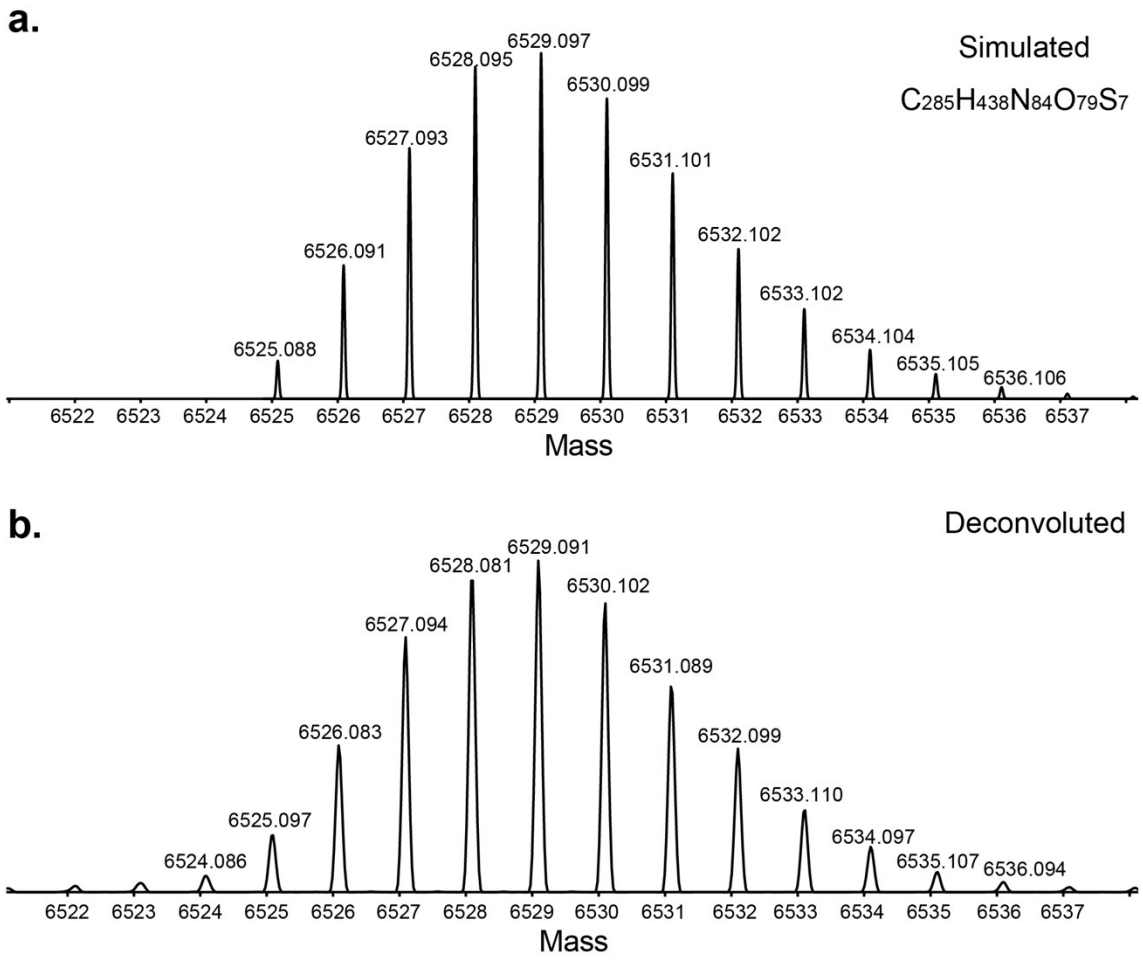

Figure S15. HR-MS analysis of reduced MT-BPTI. **a**. The simulated HR-MS of reduced MT-BPTI with chemical formula $C_{285}H_{438}N_{84}O_{79}S_7$ is shown; **b**. The deconvoluted HR-MS of reduced MT-BPTI.

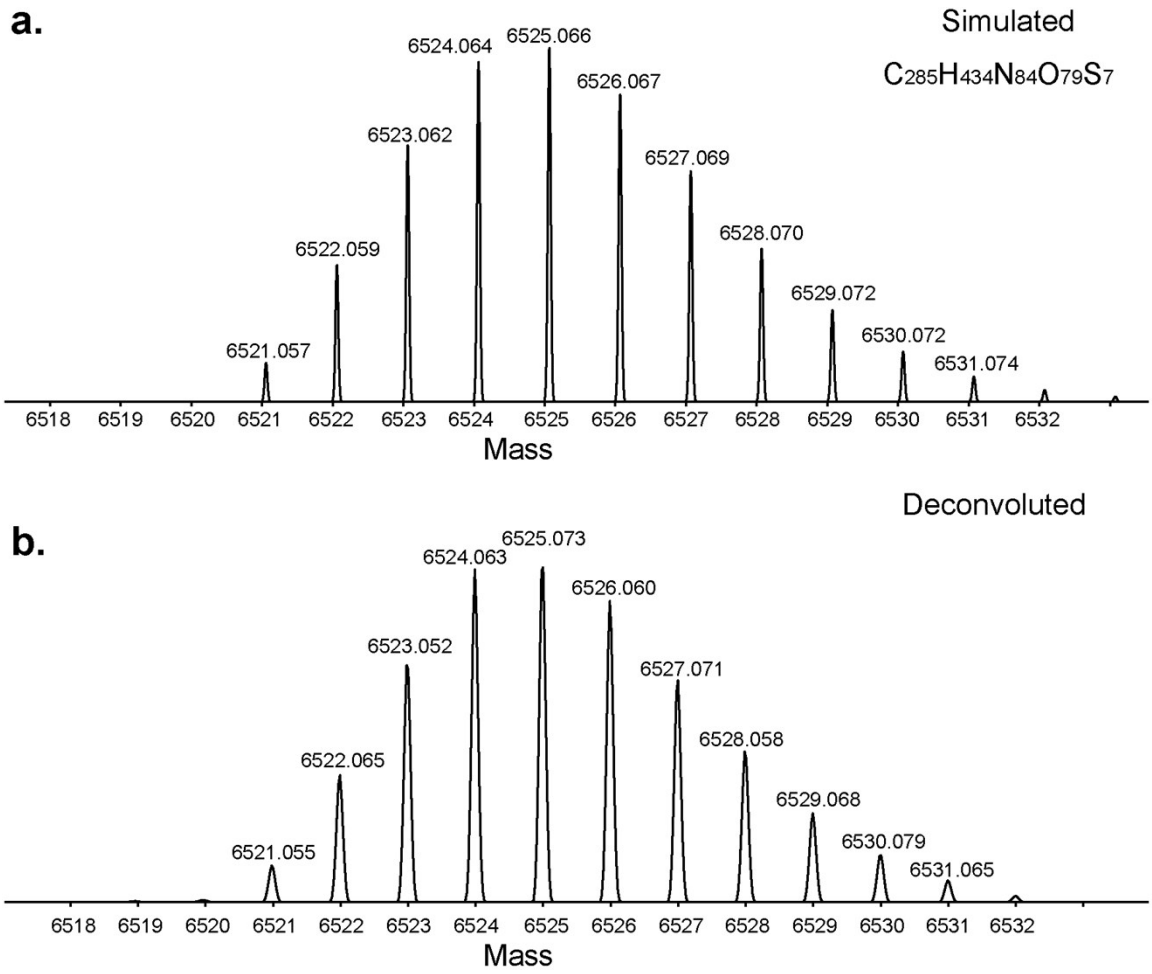

Figure S16. HR-MS analysis of folded MT-BPTI. **a**. The simulated HR-MS of reduced MT-BPTI with chemical formula $C_{285}H_{434}N_{84}O_{79}S_7$ is shown; **b**. The deconvoluted HR-MS of reduced MT-BPTI.

Bibliography

1. J. A. Mendoza, M. B. Jarstfer and D. P. Goldenberg, *Biochemistry*, 1994, **33**, 1143-1148.
2. S. A. Beeser, T. G. Oas and D. P. Goldenberg, *J. Mol. Biol.*, 1998, **284**, 1581-1596.
3. C. M. B. K. Kourra and N. Cramer, *Chem. Sci.*, 2016, **7**, 7007-7012.
4. J. S. Weissman and P. S. Kim, *Science*, 1991, **253**, 1386-1393.
5. N. Metanis and D. Hilvert, *Chem. Sci.*, 2015, **6**, 322-325.
6. N. Metanis and D. Hilvert, *Angew. Chem. Int. Ed.*, 2012, **51**, 5585-5588.
7. M. J. M. Castro and S. Anderson, *Biochemistry*, 1996, **35**, 11435-11446.
8. C. N. Pace, F. Vajdos, L. Fee, G. Grimsley and T. Gray, *Prot. Sci.*, 1995, **4**, 2411-2423.
9. J. W. Williams and J. F. Morrison, *Methods Enzym.*, 1979, **63**, 437-467.
10. W. Kabsch, *Acta Crystallogr. D.*, 2010, **66**, 125-132.
11. A. J. McCoy, R. W. Grosse-Kunstleve, P. D. Adams, M. D. Winn, L. C. Storoni and R. J. Read, *J. Appl. Crystallog.*, 2007, **40**, 658-674.
12. J. Lubkowski and A. Wlodawer, *Acta Crystallogr. D*, 1999, **55**, 335-337.
13. P. Emsley and K. Cowtan, *Acta Crystallogr. D.*, 2004, **60**, 2126-2132.
14. P. V. Afonine, R. W. Grosse-Kunstleve, N. Echols, J. J. Headd, N. W. Moriarty, M. Mustyakimov, T. C. Terwilliger, A. Urzhumtsev, P. H. Zwart and P. D. Adams, *Acta Crystallogr. D.*, 2012, **68**, 352-367.
15. R. A. Laskowski, M. W. Macarthur, D. S. Moss and J. M. Thornton, *J. Appl. Crystallogr*, 1993, **26**, 283-291.
16. V. B. Chen, W. B. Arendall, J. J. Headd, D. A. Keedy, R. M. Immormino, G. J. Kapral, L. W. Murray, J. S. Richardson and D. C. Richardson, *Acta Crystallogr. D*, 2010, **66**, 12-21.
17. P. W. Rose, C. X. Bi, W. F. Bluhm, C. H. Christie, D. Dimitropoulos, S. Dutta, R. K. Green, D. S. Goodsell, A. Prlic, M. Quesada, G. B. Quinn, A. G. Ramos, J. D. Westbrook, J. Young, C. Zardecki, H. M. Berman and P. E. Bourne, *Nucleic Acids Res*, 2013, **41**, D475-D482.